A positive feedback between weather and decadal variability and impact on frequency of extreme El Niño

1997 extreme El Niño

Wenju Cai

.. a paper under review ..

Indonesian wildfire, 1997

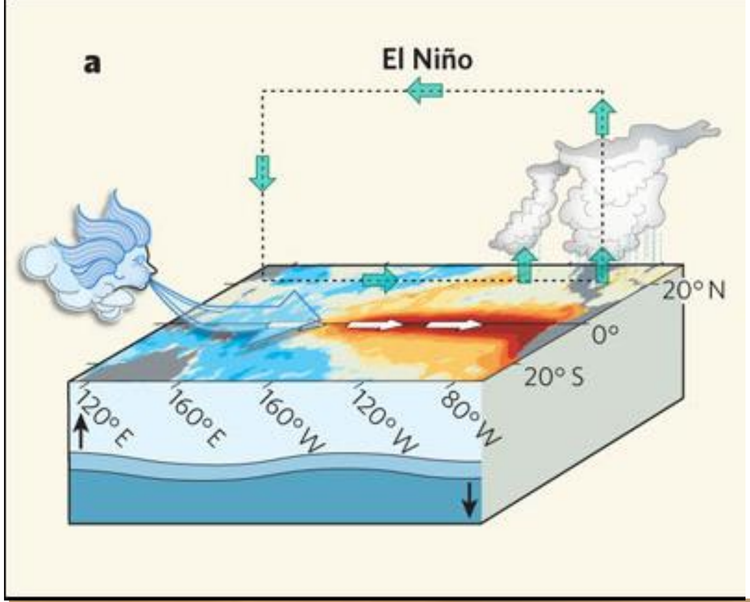

China 1998 floods, killing 1000s, and displacing 250m

Characteristics of extreme El Niño events on seasonal scales

1. Zonal SPCZ
2. ITCZ movement to the equator
3. Eastward propagation of SST anomalies

Aug. 2012

nature
International weekly journal of science
www.nature.com

1982/83,1997/98, 1991/92

More Extreme Swings of the South Pacific Convergence Zone Due to Greenhouse Warming

Wenju Cai, Matthieu Lengaigne, Simon Borlace, Matthew Collins, Tim Cowan, Michael J. McPhaden, Axel Timmermann, Scott Power, Josephine Brown, Christophe Menkes, Arona Ngari, Emmanuel M. Vincent and Matthew J. Widlansky

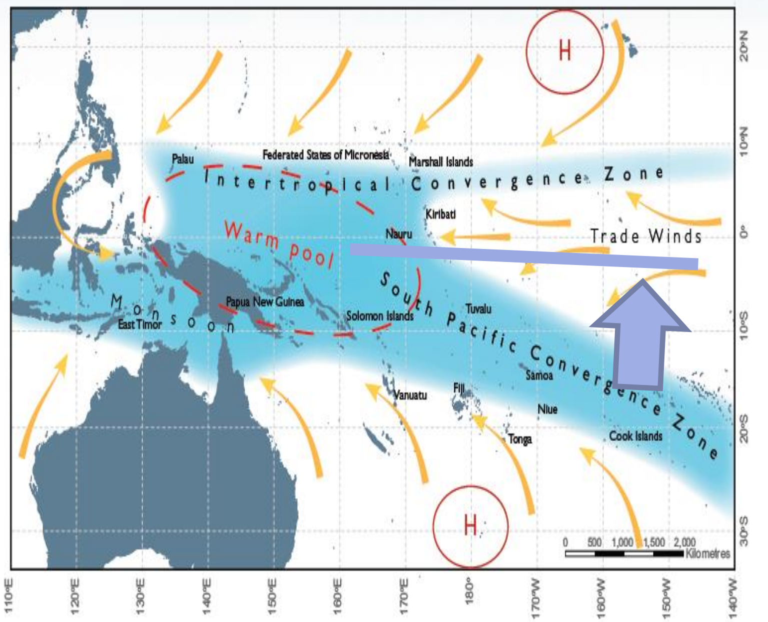

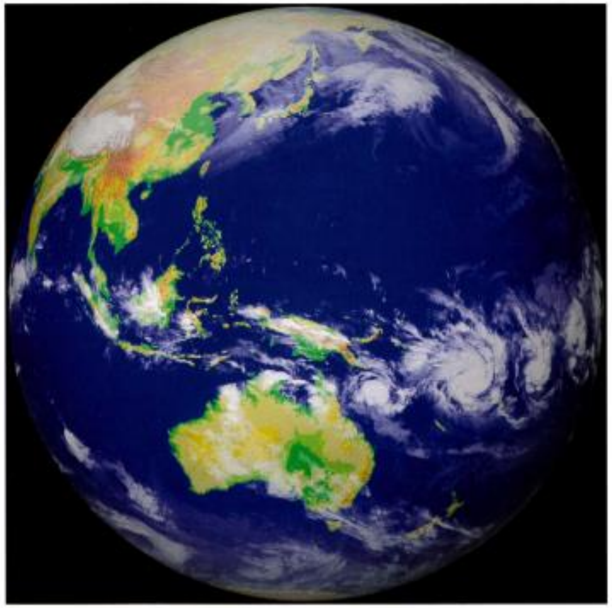

Infrared satellite image obtained with the Geostationary Meteorological Satellite-5 (or GMS5) on January, 4th. 1998 at 14:00 UTC showing three tropical cyclones (from left to right: Katrina, Susan, Ron) during the period of a zonal SPCZ event. Courtesy of IIS, University of Tokyo, processed by Japan National Institute of Informatics.

Reprinted from *Nature*, Volume 488, August 16, 2012

npg

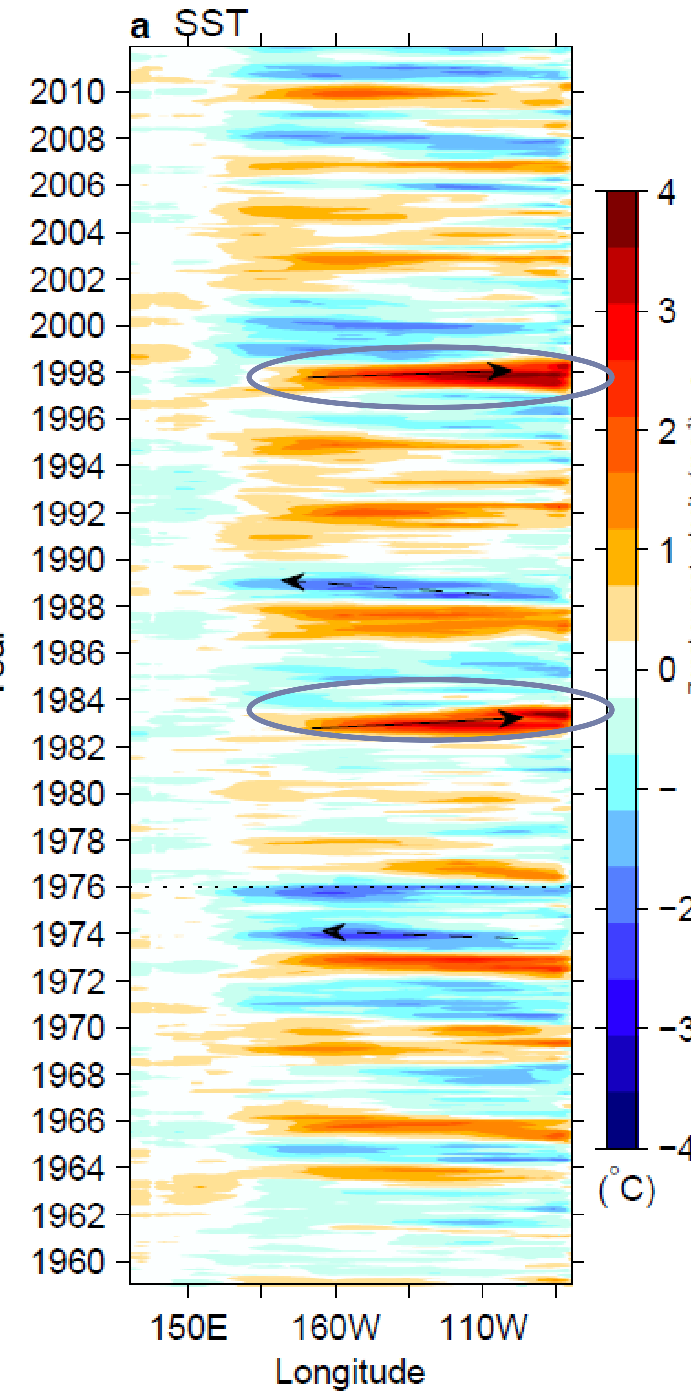

LETTER

Nov. 2013

doi:10.1038/nature12683

Late-twentieth-century emergence of the El Niño propagation asymmetry and future projections

Agus Santoso[1], Shayne McGregor[1], Fei-Fei Jin[2], Wenju Cai[3], Matthew H. England[1], Soon-Il An[4], Michael J. McPhaden[5] & Eric Guilyardi[6,7]

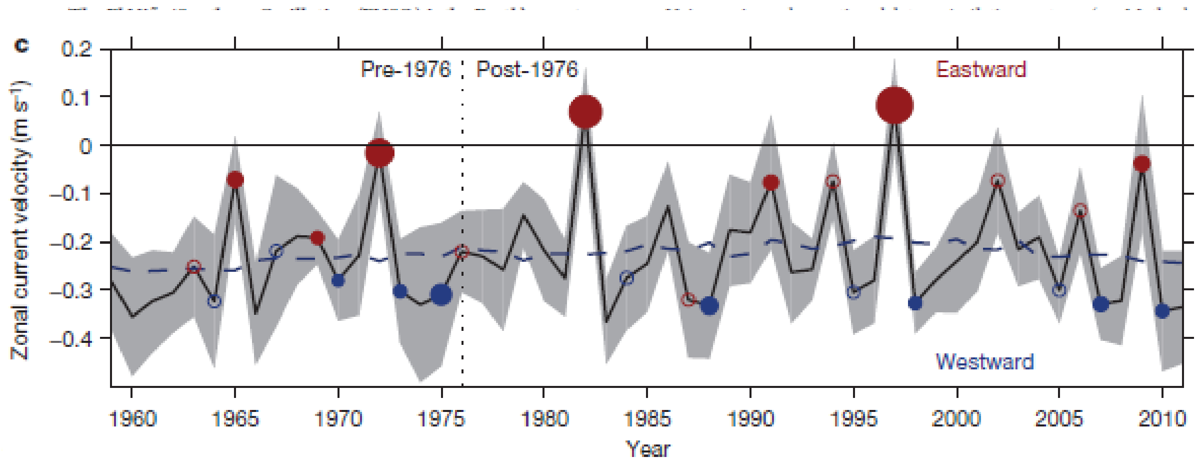

warmer world. Our a
gence of propagation
warming climate.

The tropical Pacific i
thermal and dynamica
overlying atmosphere[1]
during extreme El Niñ
Extended Data Fig. 1a)
intensify the anomalou
pool (water with tempe
the eastern edge of the v
ward shift of equatoria
Hemisphere's largest r
causing extreme hydroc
rable island countries i
continent felt the impa
the 1982–83 extreme E
were estimated to be a
billion in 2013 dollars)

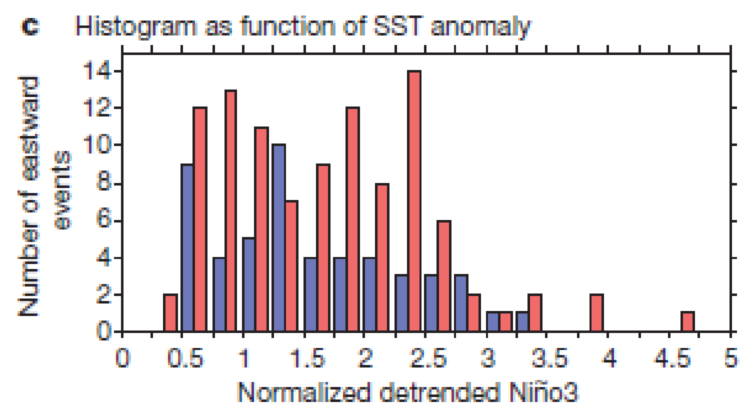

stood as arising from
s[17,18]. The zonal advec-
ith fluctuations in the
SST along the Equator
(w^a)[20,21], respectively
overbar indicates cli-
nomaly. The thermo-
/dz)[a]) associated with
nce SST in the eastern
at the thermocline (a
re gradients below the
gation of SST anoma-
e feedback dominates,
highlighted a higher
ecades since the mid-
rd propagation during
ions[10] (Fig. 1b).
cement of the prevai-
rface currents. On the

These profound impacts demand an improved understanding of ENSO propagation dynamics. Many studies have evaluated the relative importance of various ocean–atmosphere feedback processes[17–19], yet the mechanism for the propagation asymmetry remains unresolved. Here we show that an asymmetry in the zonal flow along the equatorial Pacific upper ocean (hereafter referred to as the equatorial Pacific current) is the main cause.

other hand, eastward current anomalies during El Niño associated with anomalously weak trade winds[24] (Extended Data Fig. 2), oppose and even exceed in amplitude the background current, leading to a net eastward flow (Fig. 1c). This asymmetry in the total zonal current is apparent in all reanalyses (Extended Data Fig. 3, Supplementary Tables 2 and 3). Our heat budget analysis (see Methods) shows that advection of anomalous temperature by the total current, $(\bar{u}+u^a)(dT/dx)^a$,

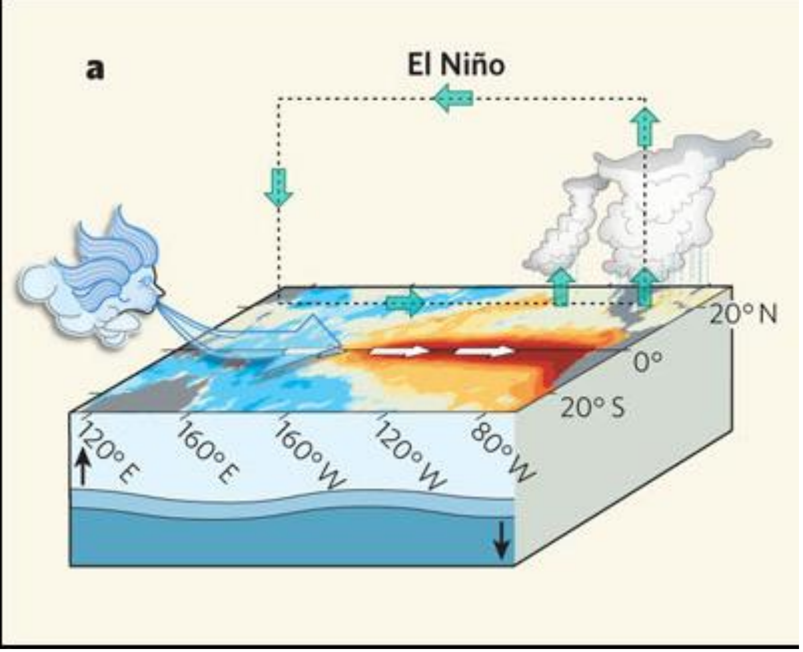

Extreme El Niño

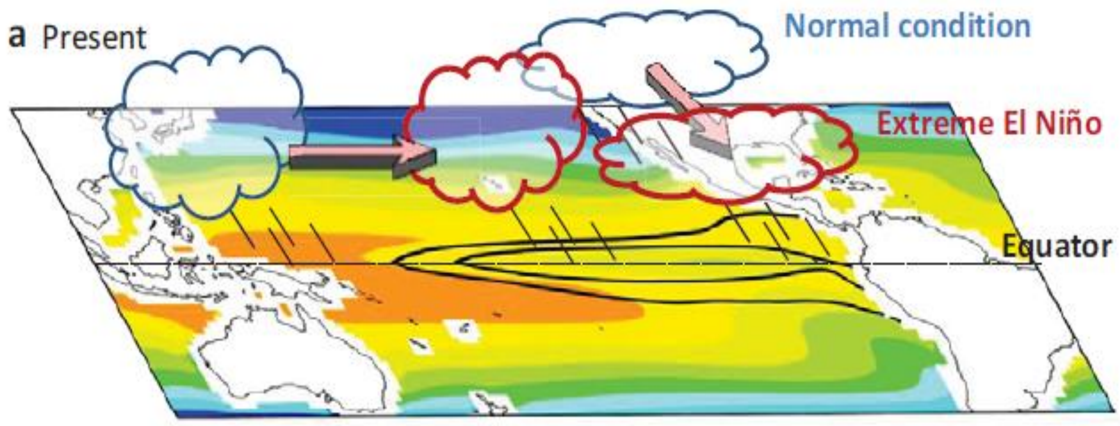

nature climate change

LETTERS

PUBLISHED ONLINE: 19 JANUARY 2014 | DOI: 10.1038/NCLIMATE2100

Jan. 2014

Increasing frequency of extreme El Niño events due to greenhouse warming

Wenju Cai[1,2]*, Simon Borlace[1], Matthieu Lengaigne[3], Peter van Rensch[1], Mat Collins[4], Gabriel Vecchi[5], Axel Timmermann[6], Agus Santoso[7], Michael J. McPhaden[8], Lixin Wu[2], Matthew H. England[7], Guojian Wang[1,2], Eric Guilyardi[3,9] and Fei-Fei Jin[10]

El Niño events are a prominent feature of climate variability with global climatic impacts. The 1997/98 episode, often referred to as 'the climate event of the twentieth century'[1,2], and the 1982/83 extreme El Niño[3], featured a pronounced eastward extension of the west Pacific warm pool and development of atmospheric convection, and hence a huge rainfall increase, in the usually cold and dry equatorial eastern Pacific. Such a massive reorganization of atmospheric convection, which we define as an extreme El Niño, severely disrupted global weather patterns, affecting ecosystems[4,5], agriculture[6], tropical cyclones, drought, bushfires, floods and other extreme weather events worldwide[3,7–9]. Potential future changes in such extreme El Niño occurrences could have profound socio-economic consequences. Here we present climate modelling evidence for a doubling in the occurrences in the future in response to greenhouse warming. We estimate the change by aggregating results from climate models in the Coupled Model Intercomparison Project phases 3 (CMIP3; ref. 10) and 5 (CMIP5; ref. 11) multi-model databases, and

extended to every continent, and the 1997/98 event alone caused US$35–45 billion in damage and claimed an estimated 23,000 human lives worldwide[17].

The devastating impacts demand an examination of whether greenhouse warming will alter the frequency of such extreme El Niño events. Although many studies have examined the effects of a projected warming on the Pacific mean state, El Niño diversity and El Niño teleconnections[18–21], the issue of how extreme El Niños will change has not been investigated. Here we show that greenhouse warming leads to a significant increase in the frequency of such events.

We contrast the characteristics between the extreme and moderate El Niño events using available data sets[22,23], focusing on December–January–February (DJF), the season in which El Niño events peak. During moderate events, which include canonical and Modoki El Niño[24], the eastern boundary of the warm pool (indicated by the 28 °C isotherm, purple, Fig. 1a) and the atmospheric convective zone move eastwards to just east of the Date Line. The ITCZ lies north of the Equator[25]

nature climate change

LETTERS

PUBLISHED ONLINE: 26 JANUARY 2015 | DOI: 10.1038/NCLIMATE2492

Jan. 2015

Increased frequency of extreme La Niña events under greenhouse warming

Wenju Cai[1,2]*, Guojian Wang[1,2], Agus Santoso[3], Michael J. McPhaden[4], Lixin Wu[2], Fei-Fei Jin[5], Axel Timmermann[6], Mat Collins[7], Gabriel Vecchi[8], Matthieu Lengaigne[9], Matthew H. England[3], Dietmar Dommenget[10], Ken Takahashi[11] and Eric Guilyardi[9,12]

The El Niño/Southern Oscillation is Earth's most prominent source of interannual climate variability, alternating irregularly between El Niño and La Niña, and resulting in global disruption of weather patterns, ecosystems, fisheries and agriculture[1–5]. The 1998–1999 extreme La Niña event that followed the 1997–1998 extreme El Niño event[6] switched extreme El Niño-induced severe droughts to devastating floods in western Pacific countries, and vice versa in the southwestern United States[4,7]. During extreme La Niña events, cold sea surface conditions develop in the central Pacific[8,9], creating an enhanced temperature gradient from the Maritime continent to the central Pacific. Recent studies have revealed robust changes in El Niño characteristics in response to simulated future greenhouse warming[10–12], but how La Niña will change remains unclear. Here we present climate modelling evidence, from simulations conducted for the Coupled Model

1998, extreme events occurred, in part linked to the developing 1998–1999 La Niña event. The southwestern United States experienced one of the most severe droughts in history[4,7,18]. Venezuela endured flash flooding and landslides that killed 25,000 to 50,000 people[19]. In China, river floods and storms led to the death of thousands, and displaced over 200 million people[20]. Bangladesh experienced one of the most destructive flooding events in modern history, with over 50% of the country's land area flooded, leading to severe food shortages and the spread of waterborne epidemic diseases, killing several thousand people and affecting over 30 million more[21–23]. The 1998 North Atlantic hurricane season saw one of the deadliest and strongest hurricanes (Mitch) in the historical record[4], claiming more than 11,000 lives in Honduras and Nicaragua[24].

The 1998–1999 La Niña event occurred after the 1997–1998 extreme El Niño event—referred to as the climate event of the twentieth century[3], inducing swings of opposite extremes from one

Characteristics of extreme El Niño events on seasonal scales

1. Zonal SPCZ
2. ITCZ movement to the equator
3. Eastward propagation of SST anomalies

Characteristics of extreme El Niño events on weather scales

1. WWEs

NCEP data

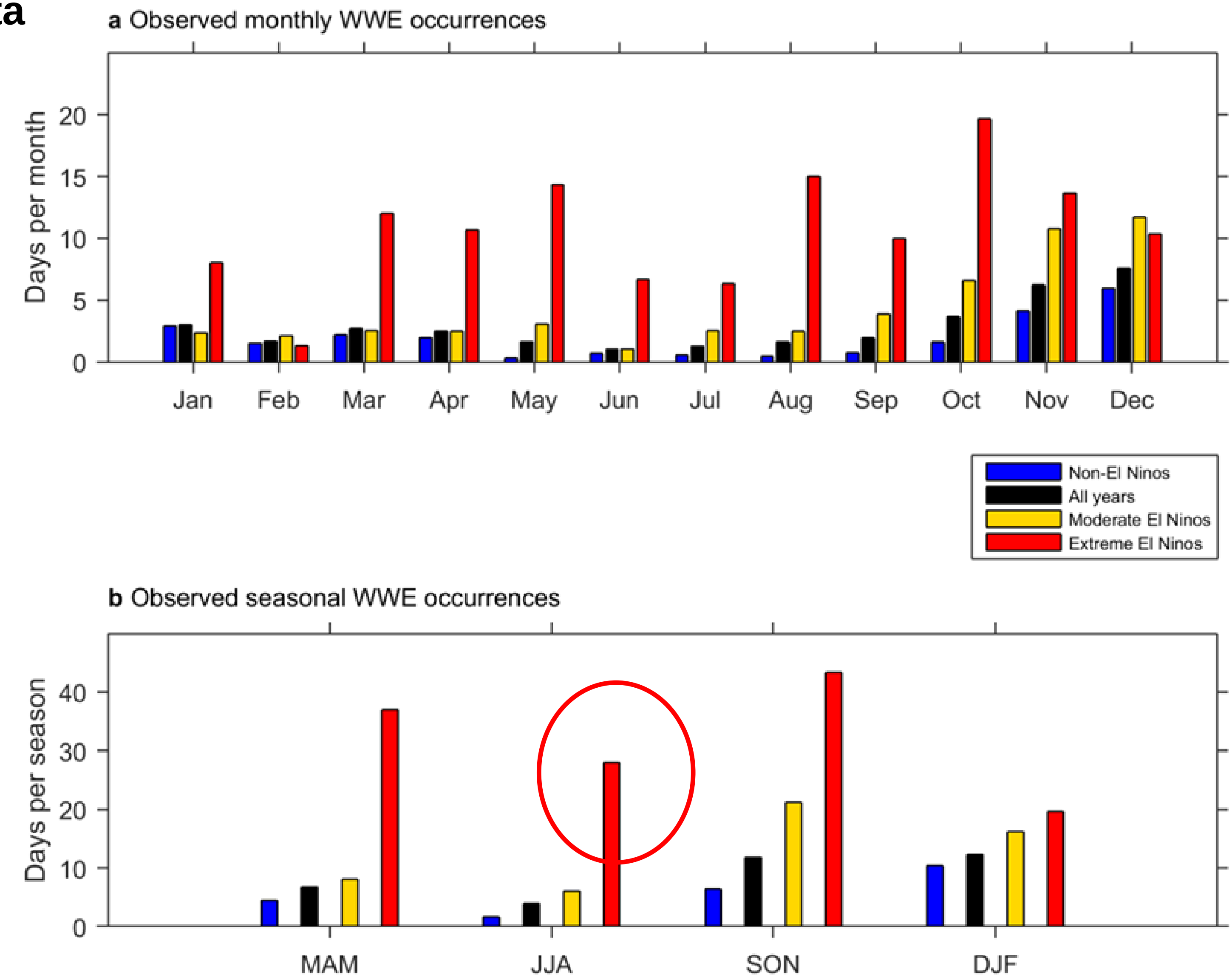
a Observed monthly WWE occurrences
Days per month
0
5
10
15
20
Jan
Feb
Mar
Apr
May
Jun
Jul
Aug
Sep
Oct
Nov
Dec
Non-El Ninos
All years
Moderate El Ninos
Extreme El Ninos
b Observed seasonal WWE occurrences
Days per season
0
10
20
30
40
MAM
JJA
SON
DJF

What the WWEs do?

- Generate downing Kelvin waves that
  - drive strong eastward currents that displace the western Pacific warm pool and convection eastward
  - reduce equatorial upwelling in the eastern Pacific, and
  - deepen the eastern equatorial Pacific thermocline

The combined effect is warming and convective anomalies that extend eastward, and in turn promote subsequent WWEs (**WWE-SST coupled positive feedback**)

Kessler et al. 1995; McPhaden 2002, McPhaden 1999; Vecchi & Harrison 2000; Lengaigne et al. 2003; Eisenman et al. 2005;Gebbie et al. 2007; Chen et al. 2015

Characteristics of extreme El Niño events on seasonal scales

1. Zonal SPCZ
2. ITCZ movement to the equator
3. Eastward propagation of SST anomalies

Characteristics of extreme El Niño events on weather scales

1. WWEs
2. Southwest Pacific southerly surges

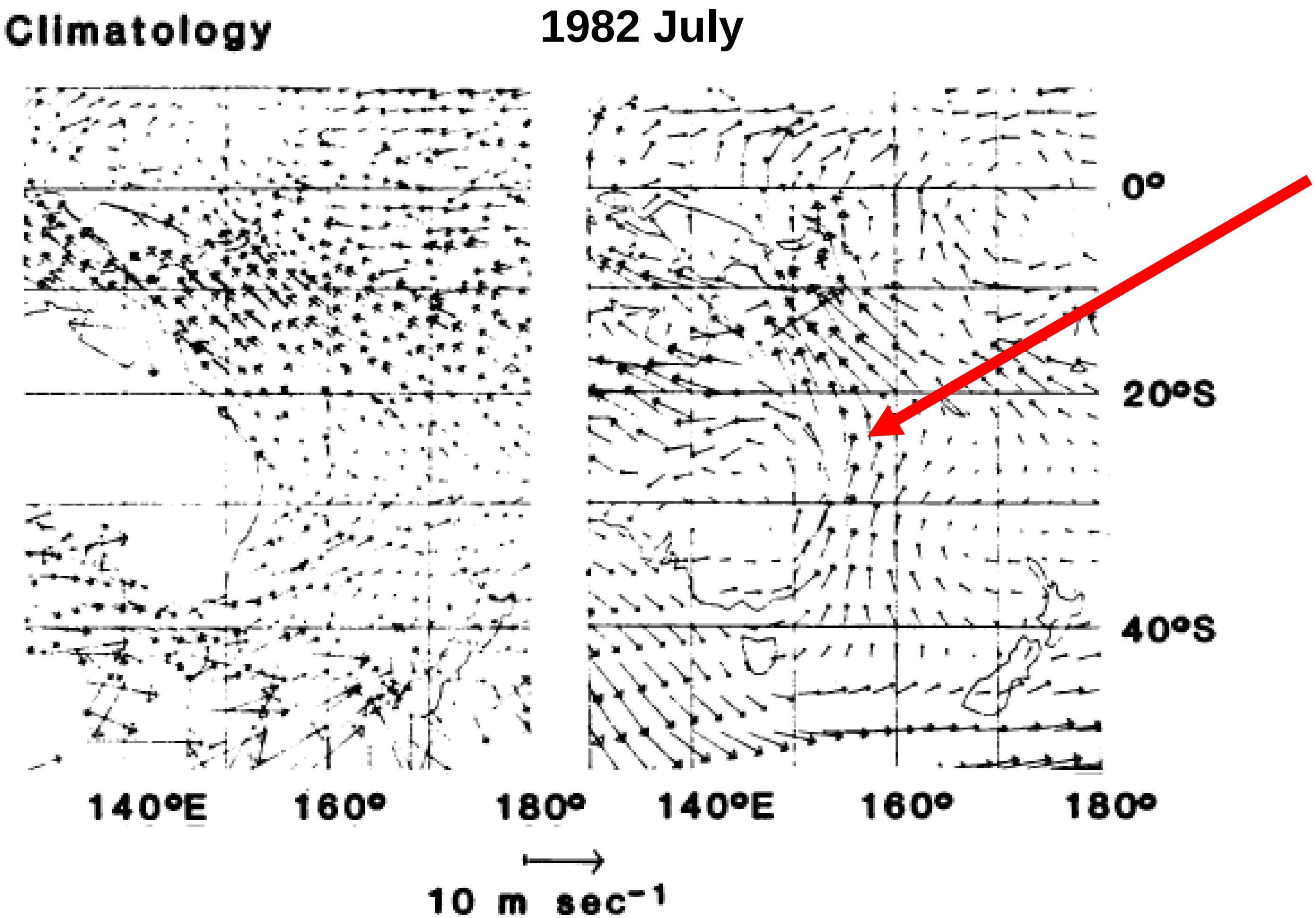

Harrison 1984, Science

Super El Niño

Moderate El Niño

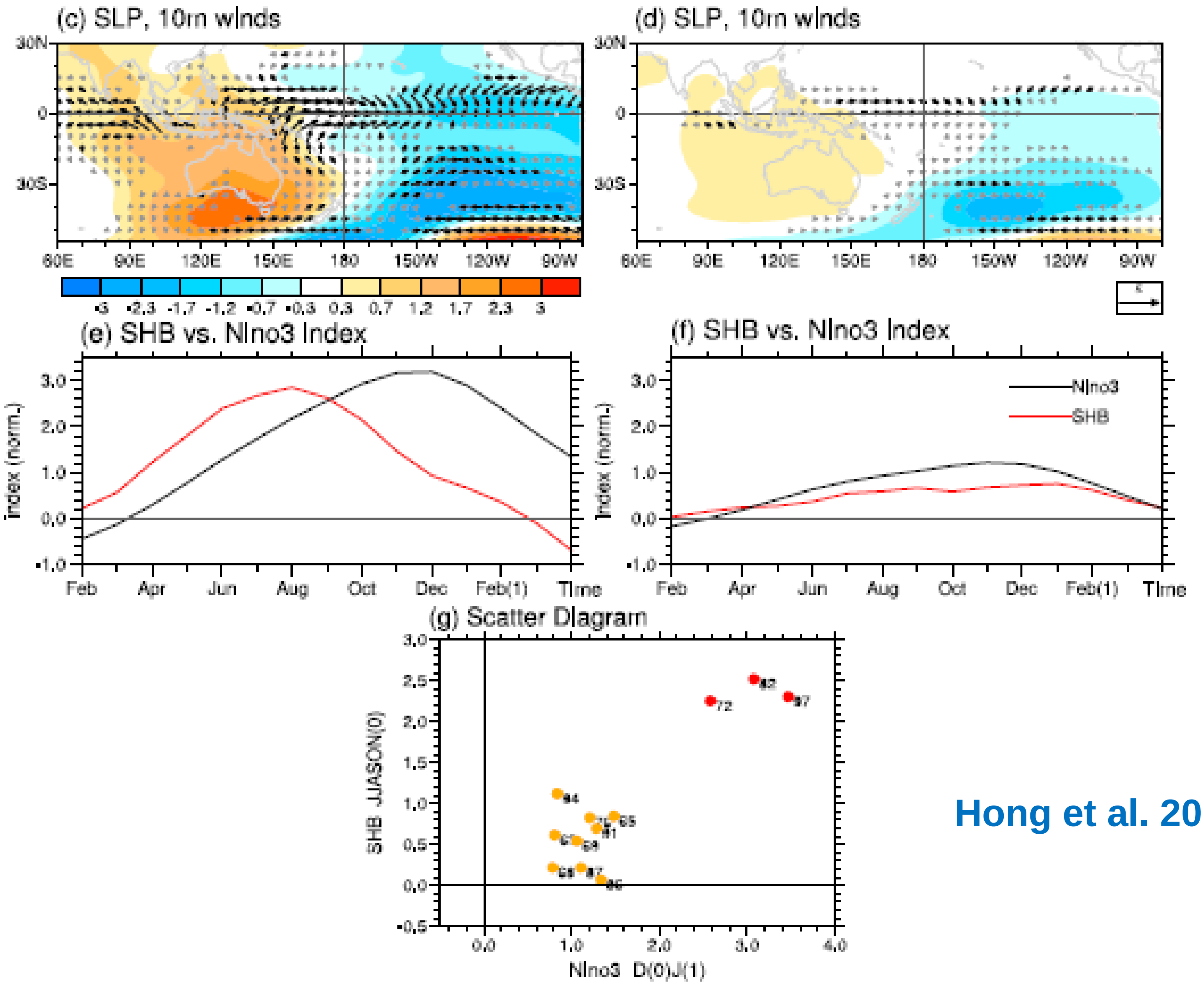

Hong et al. 2014

Relationship between decadal variability and weathers

Decadal variability in the Pacific

- Apart from the PDO, there is the tropical decadal variability (TPDV)
- TPDV is a result of rectification, associated with ENSO nonlinearity

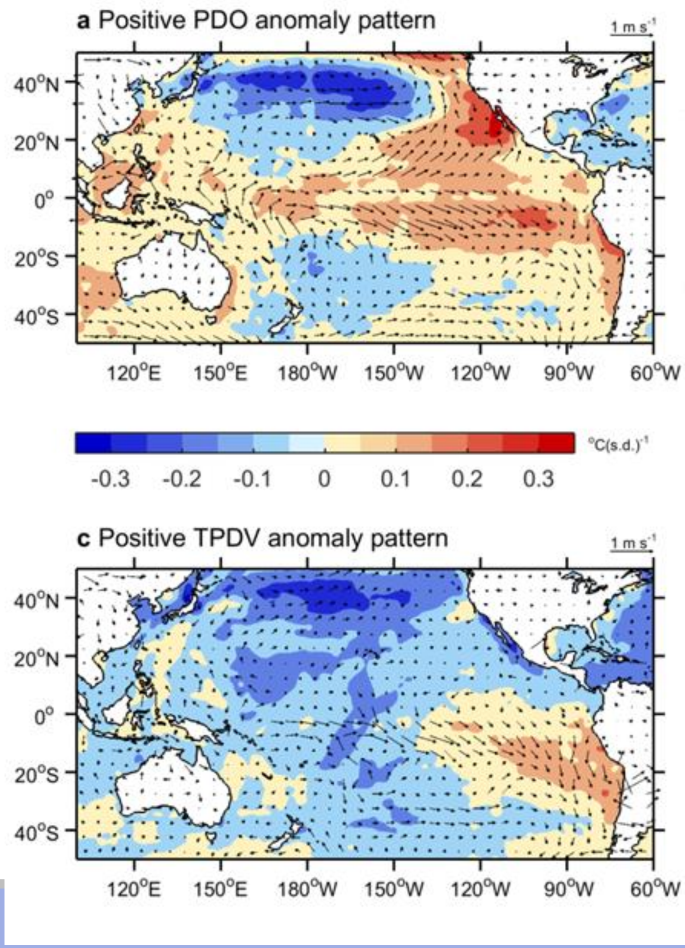

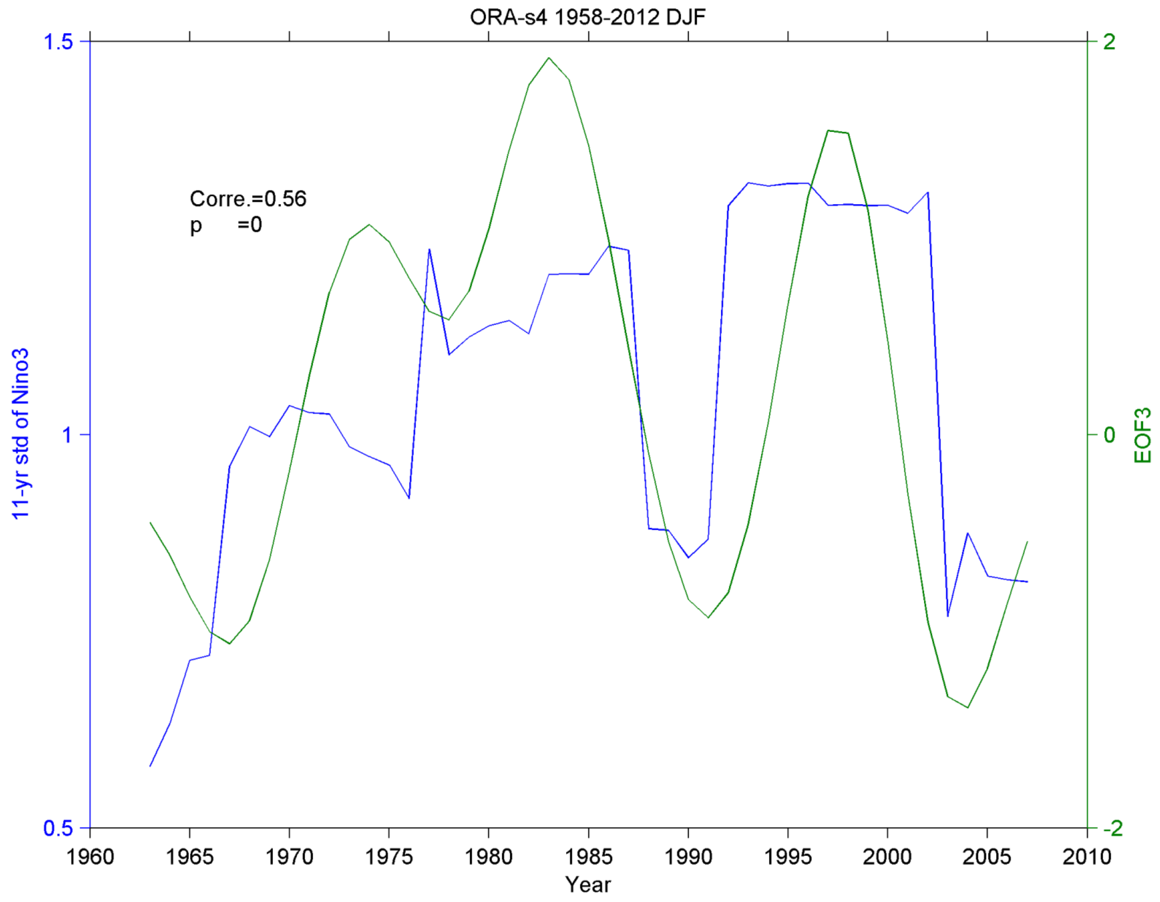

Rogers et al. 2004; Yeh & Kirtman 2004; Choi et al. 2009

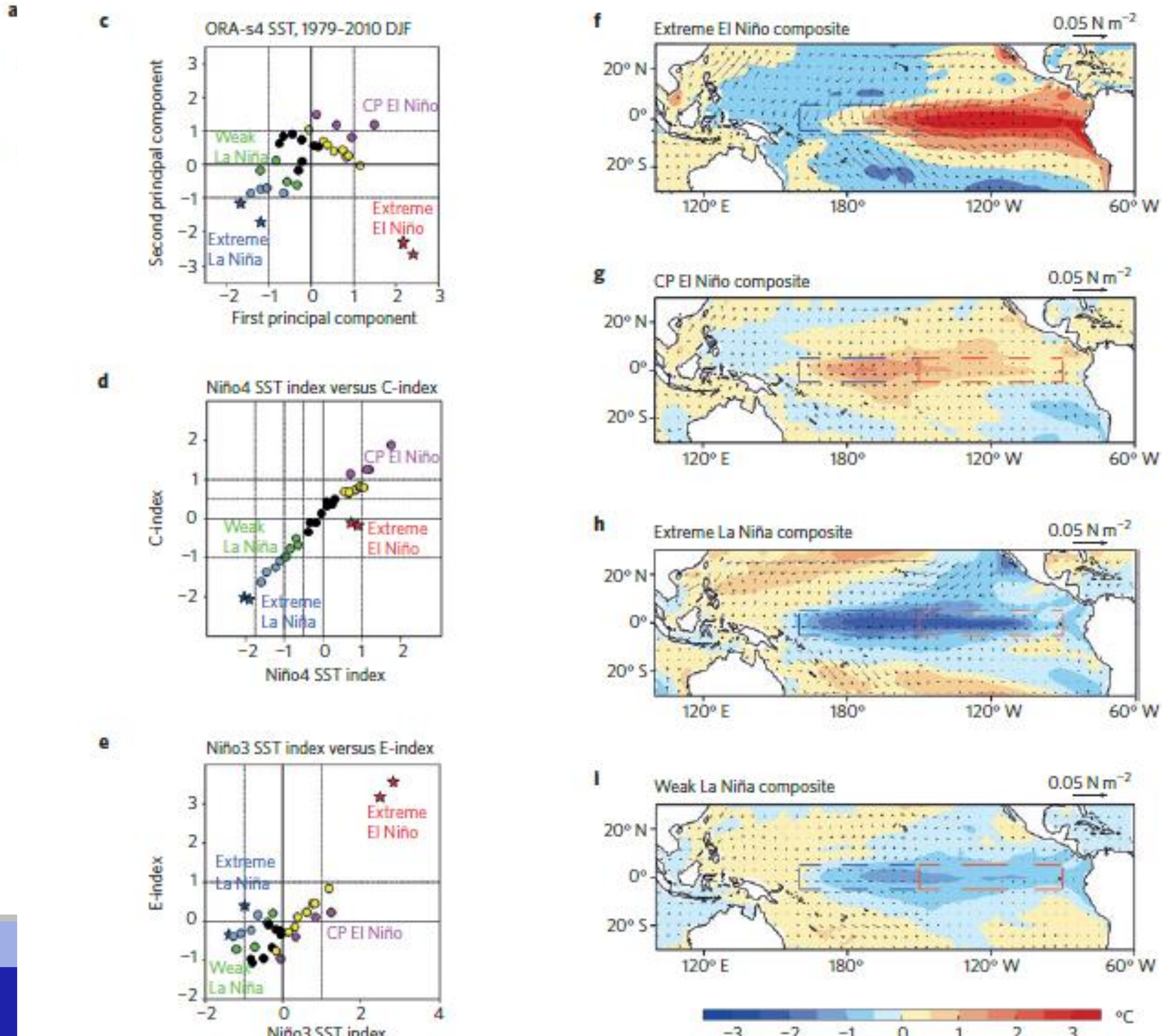
a
c
ORA-s4 SST, 1979–2010 DJF
Second principal component
First principal component
CP El Niño
Weak La Niña
Extreme El Niño
Extreme La Niña
d
Niño4 SST index versus C-index
C-index
Niño4 SST index
CP El Niño
Weak La Niña
Extreme El Niño
Extreme La Niña
e
Niño3 SST index versus E-index
E-index
Niño3 SST index
Extreme El Niño
Extreme La Niña
CP El Niño
Weak La Niña
f
Extreme El Niño composite
0.05 N m⁻²
g
CP El Niño composite
0.05 N m⁻²
h
Extreme La Niña composite
0.05 N m⁻²
i
Weak La Niña composite
0.05 N m⁻²
20° N
0°
20° S
120° E
180°
120° W
60° W
°C

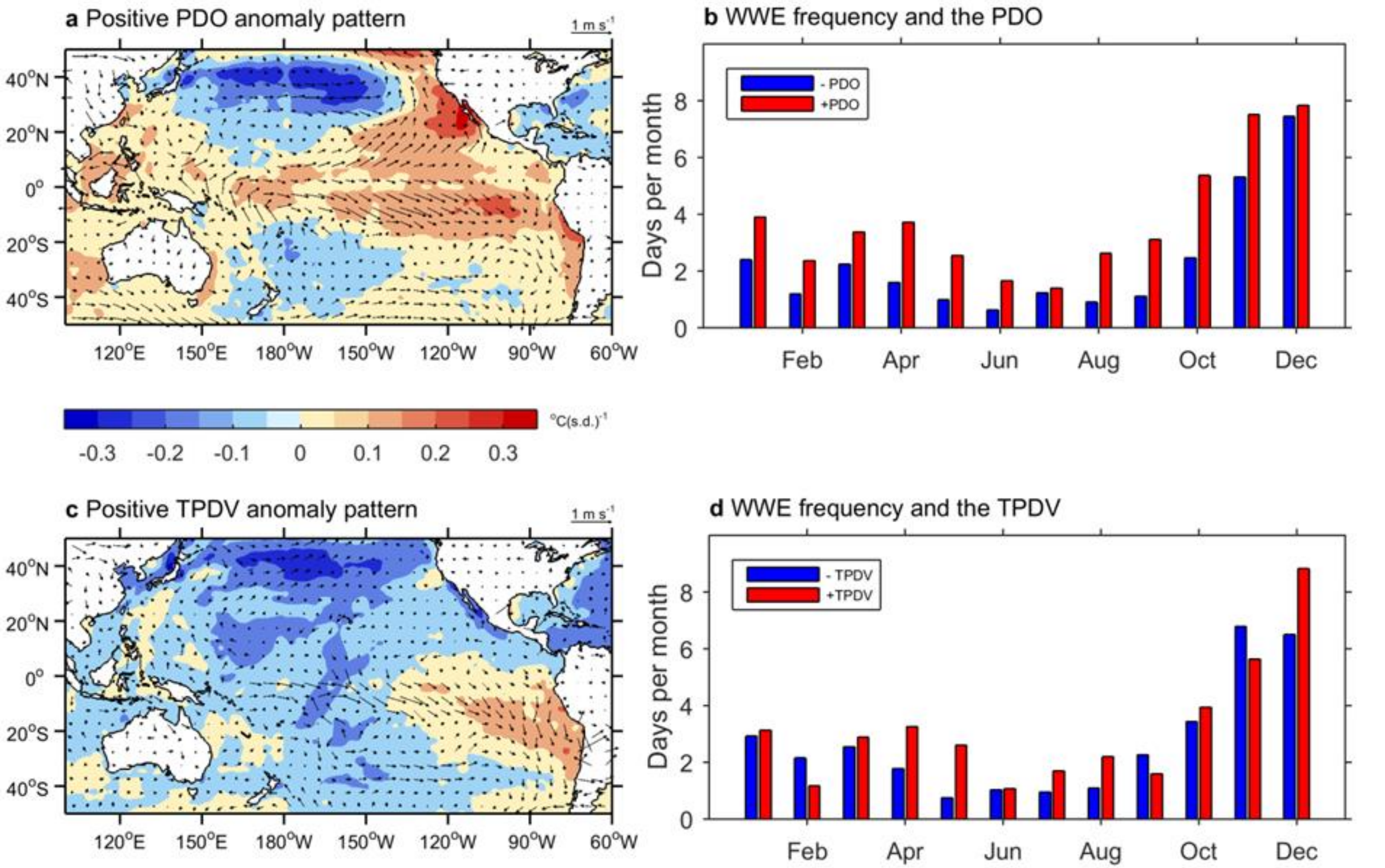
a Positive PDO anomaly pattern
b WWE frequency and the PDO
- PDO
+PDO
Days per month
Feb
Apr
Jun
Aug
Oct
Dec
40°N
20°N
0°
20°S
40°S
120°E
150°E
180°W
150°W
120°W
90°W
60°W
1 m s-1
°C(s.d.)-1
-0.3
-0.2
-0.1
0
0.1
0.2
0.3
c Positive TPDV anomaly pattern
d WWE frequency and the TPDV
- TPDV
+TPDV

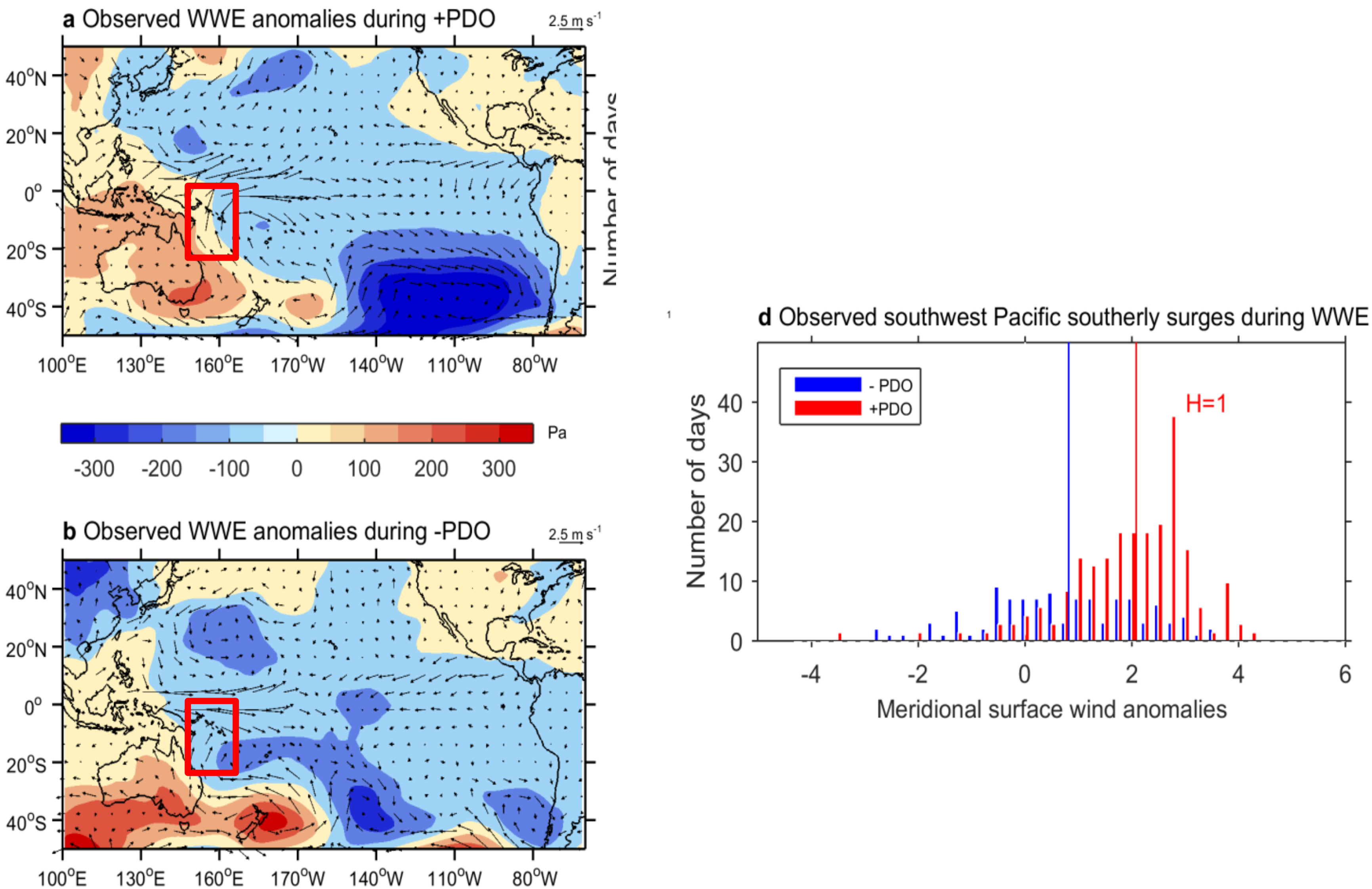
a Observed WWE anomalies during +PDO
2.5 m s-1
40°N
20°N
0°
20°S
40°S
100°E
130°E
160°E
170°W
140°W
110°W
80°W
Pa
-300
-200
-100
0
100
200
300
b Observed WWE anomalies during -PDO
d Observed southwest Pacific southerly surges during WWE
- PDO
+PDO
H=1
Number of days
Meridional surface wind anomalies
-4
-2
0
2
4
6
10
20
30
40

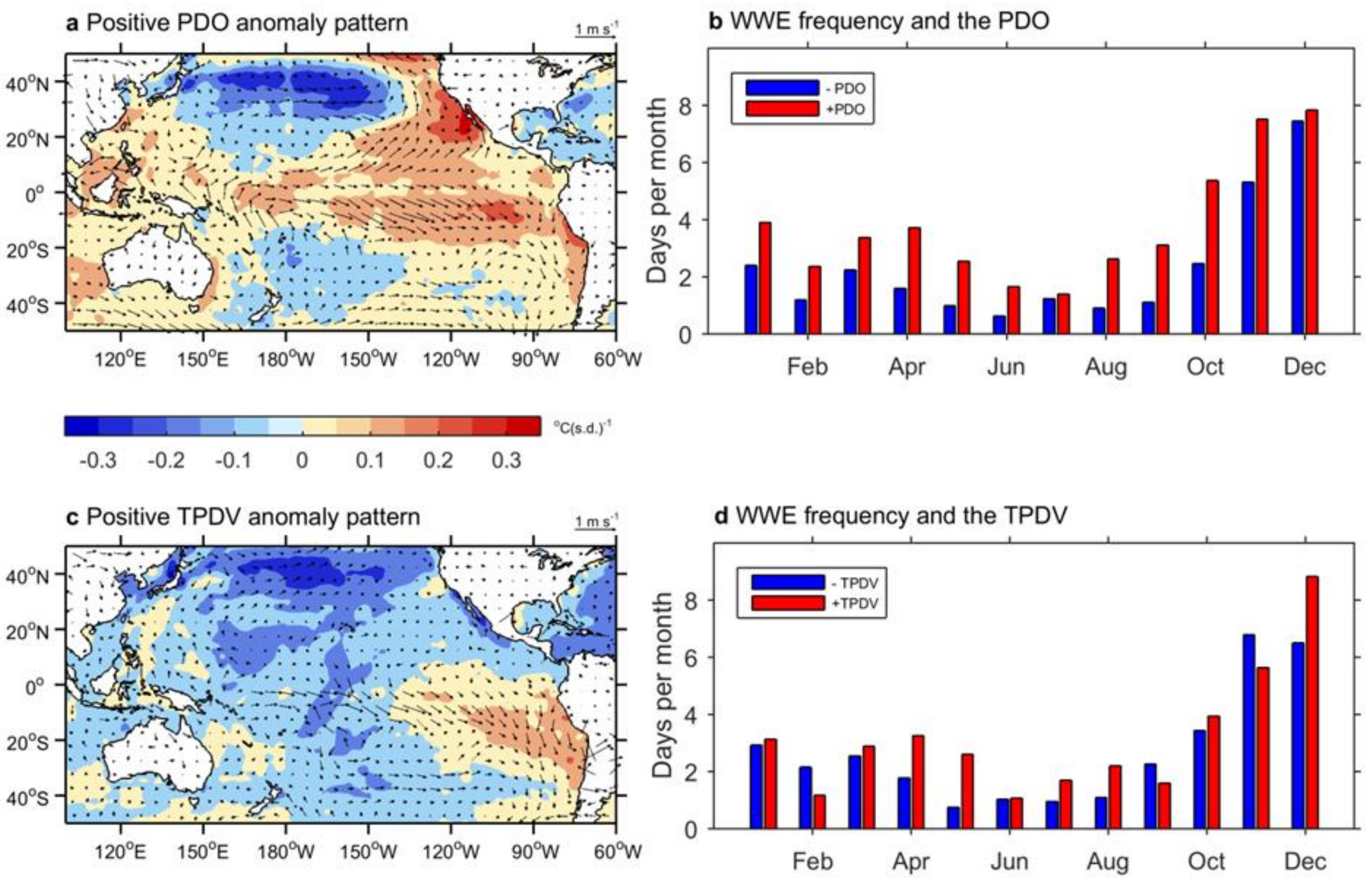
a Positive PDO anomaly pattern
b WWE frequency and the PDO
- PDO
+PDO
Days per month
Feb
Apr
Jun
Aug
Oct
Dec
c Positive TPDV anomaly pattern
d WWE frequency and the TPDV
- TPDV
+TPDV
°C(s.d.)-1
1 m s-1
-0.3
-0.2
-0.1
0
0.1
0.2
0.3
40°N
20°N
0°
20°S
40°S
120°E
150°E
180°W
150°W
120°W
90°W
60°W

Is there a relationship between WWEs and decadal variability?

Using ACCESS for five sets of experiments forcing the atmosphere with SST

- **CLIM** seasonal cycle
- CLIM + **+PDO*X**
- CLIM + **-PDO*X**

- CLIM + **+TPDV*X**
- CLIM+ **-TPDV*X**

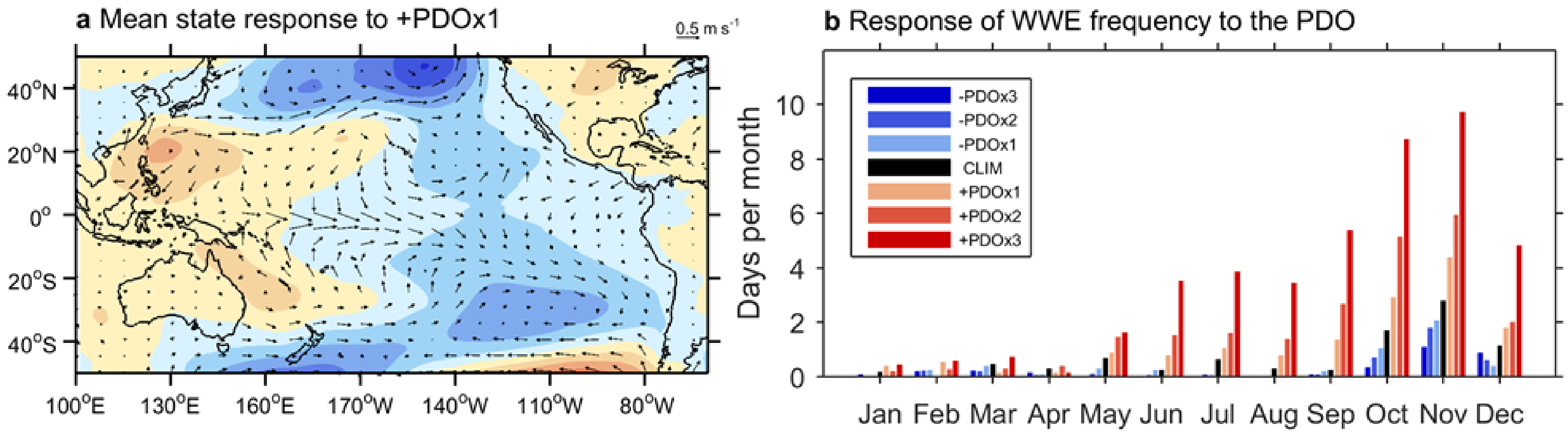

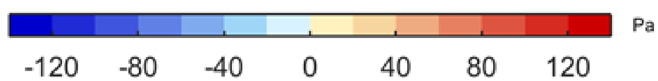

+ TPDV tend to damp WWEs !

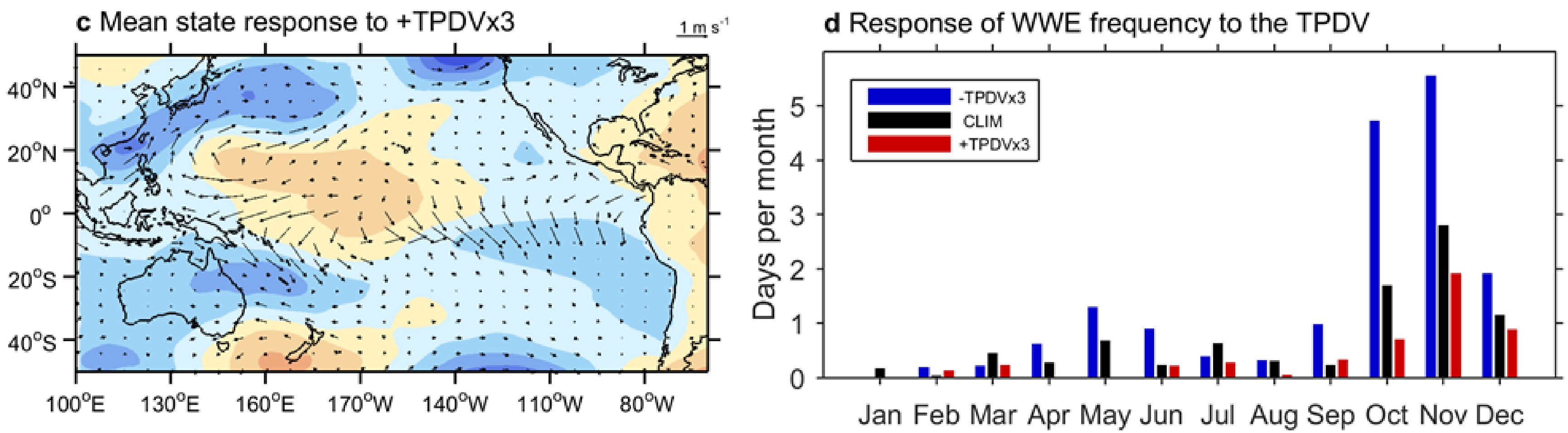

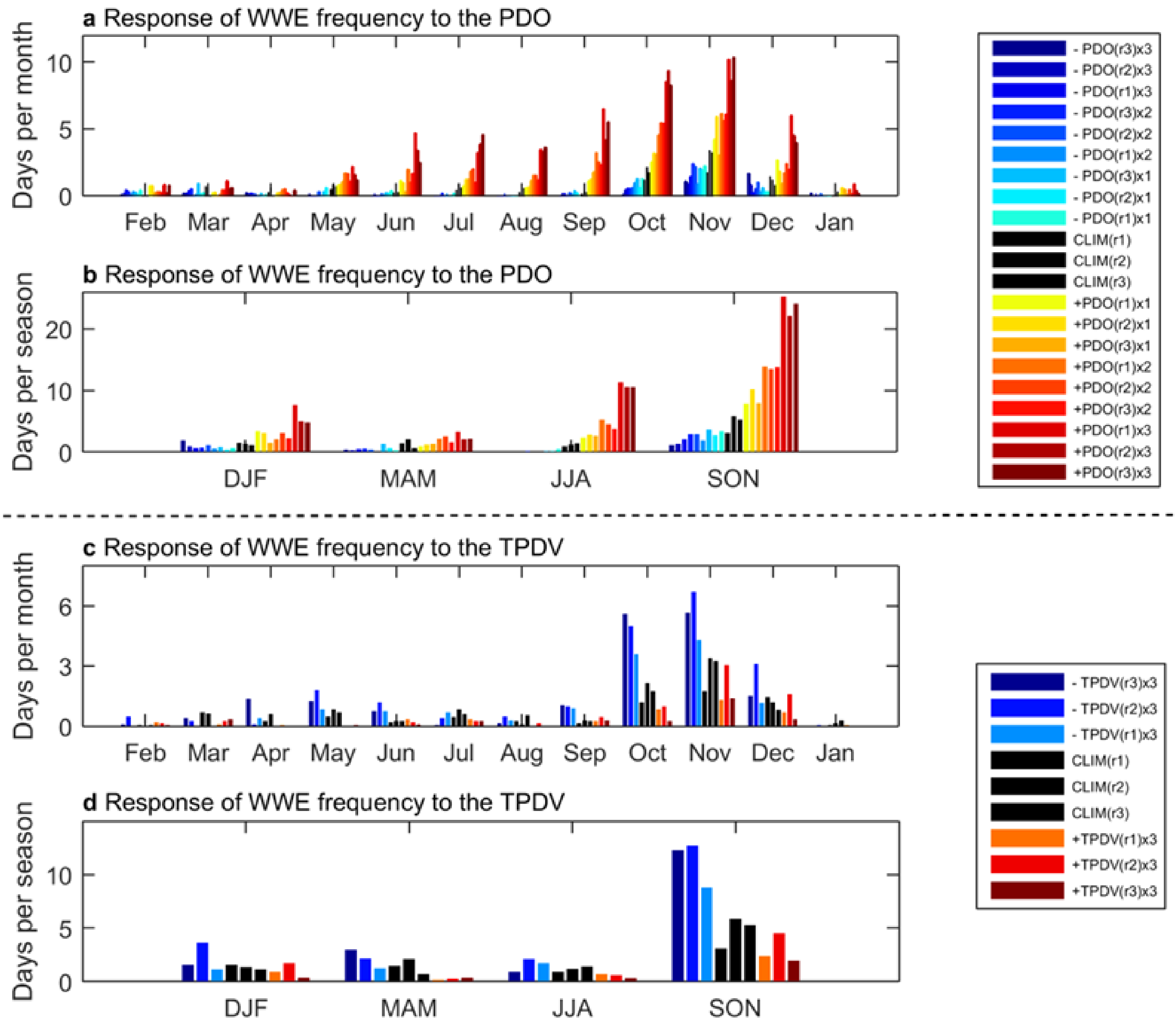
a Response of WWE frequency to the PDO
Days per month
10
5
0
Feb Mar Apr May Jun Jul Aug Sep Oct Nov Dec Jan
b Response of WWE frequency to the PDO
Days per season
20
10
0
DJF MAM JJA SON
- PDO(r3)x3
- PDO(r2)x3
- PDO(r1)x3
- PDO(r3)x2
- PDO(r2)x2
- PDO(r1)x2
- PDO(r3)x1
- PDO(r2)x1
- PDO(r1)x1
CLIM(r1)
CLIM(r2)
CLIM(r3)
+PDO(r1)x1
+PDO(r2)x1
+PDO(r3)x1
+PDO(r1)x2
+PDO(r2)x2
+PDO(r3)x2
+PDO(r1)x3
+PDO(r2)x3
+PDO(r3)x3
c Response of WWE frequency to the TPDV
Days per month
6
3
0
Feb Mar Apr May Jun Jul Aug Sep Oct Nov Dec Jan
d Response of WWE frequency to the TPDV
Days per season
10
5
0
DJF MAM JJA SON
- TPDV(r3)x3
- TPDV(r2)x3
- TPDV(r1)x3
CLIM(r1)
CLIM(r2)
CLIM(r3)
+TPDV(r1)x3
+TPDV(r2)x3
+TPDV(r3)x3

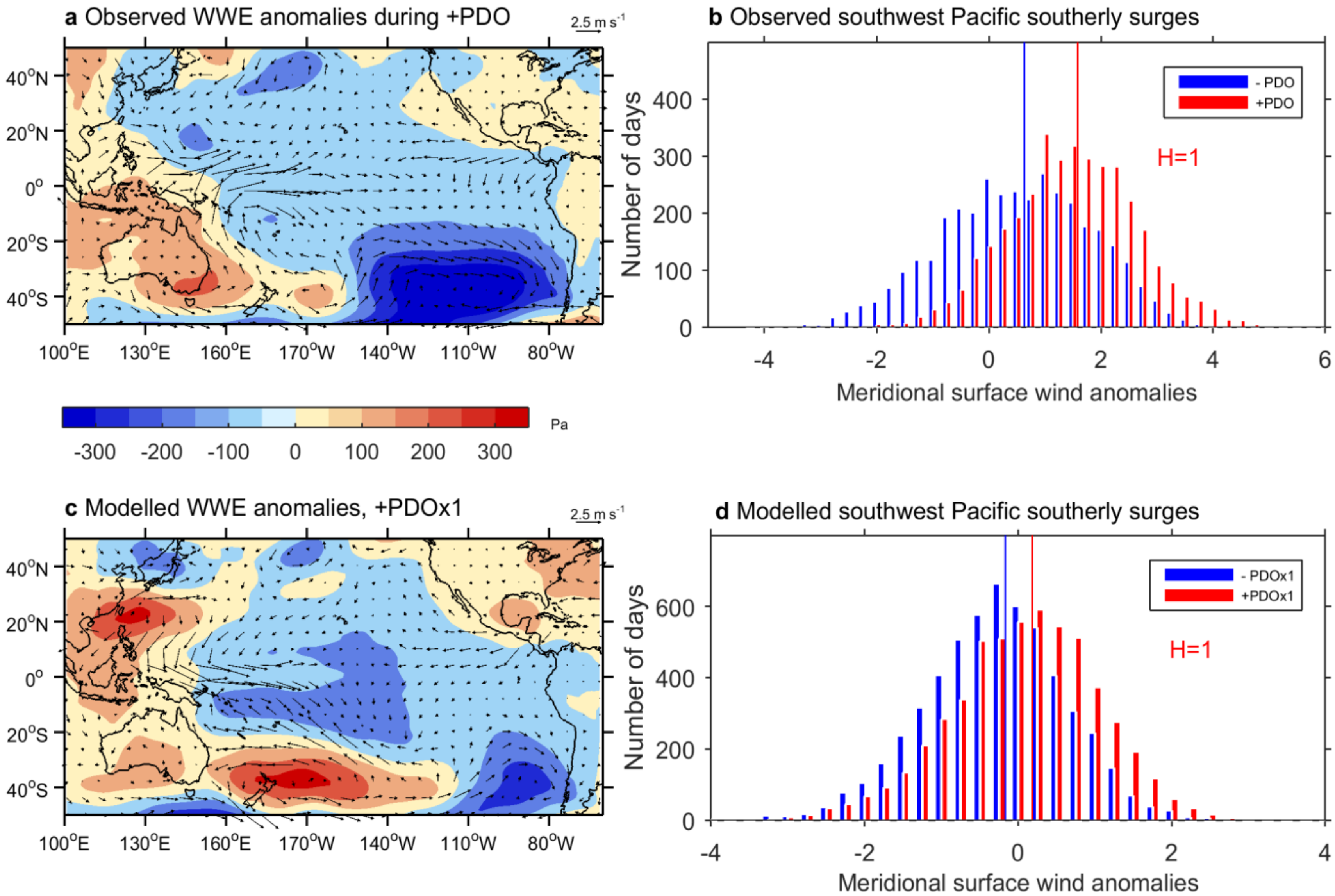
a Observed WWE anomalies during +PDO
2.5 m s-1
40°N
20°N
0°
20°S
40°S
100°E 130°E 160°E 170°W 140°W 110°W 80°W
b Observed southwest Pacific southerly surges
- PDO
+PDO
H=1
Number of days
0 100 200 300 400
-4 -2 0 2 4 6
Meridional surface wind anomalies
Pa
-300 -200 -100 0 100 200 300
c Modelled WWE anomalies, +PDOx1
2.5 m s-1
d Modelled southwest Pacific southerly surges
- PDOx1
+PDOx1
H=1
Number of days
0 200 400 600
-4 -2 0 2 4
Meridional surface wind anomalies

+PDO is conducive to WWEs; so what is the PDO?

PDO mechanism and ENSO

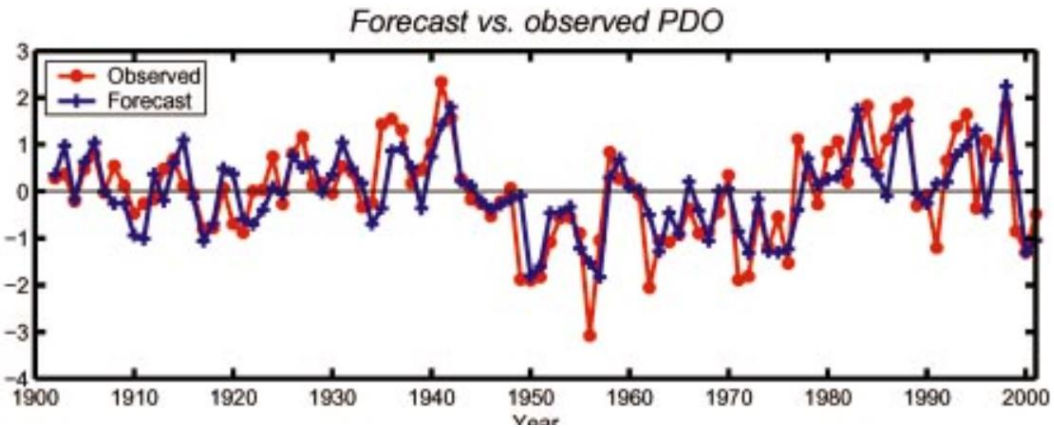

Newman et al. 2003

- Results from fluctuations of Aleutian low (Pierce et al. 2000; Alexander et al. 2002)
- Partly controlled by ENSO (Lau and Nath 1996)
- Re-emergence mechanism responsible for spectrum reddening (Deser et al. 2003)
- Accounting for these processes allow to accurately simulate PDO (Newman et al. 2003)

CSIRO

PDO mechanism continued…..

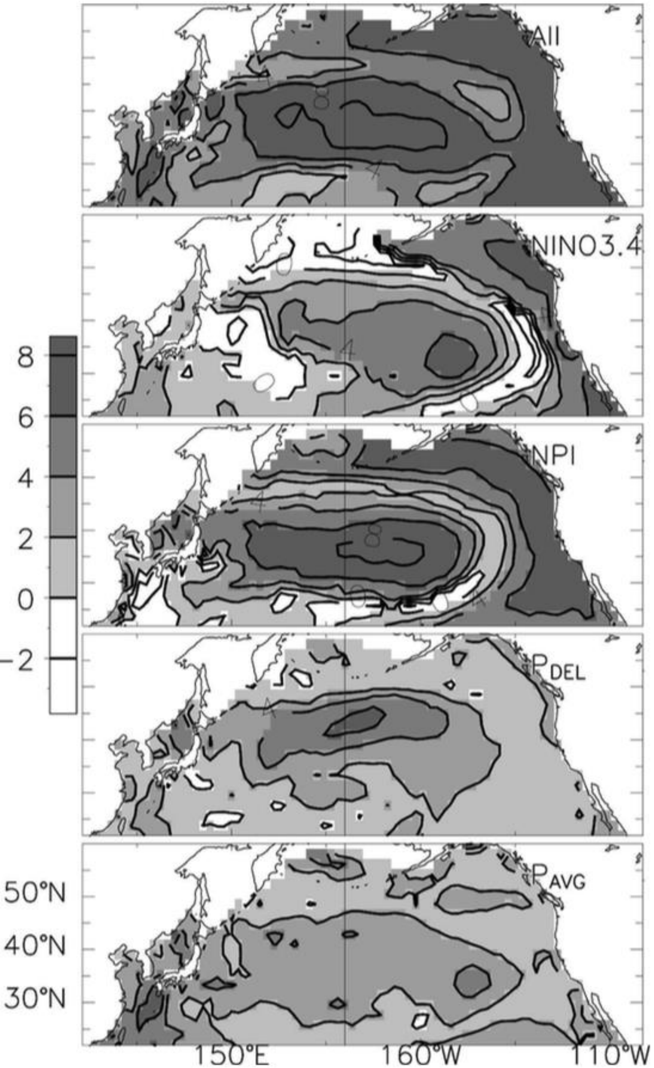

Schneider and Cornuelle 2005

Gyres fluctuations also contribute to PDO at multi-decadal timescales (Schneider and Cornuelle 2005)

PDO not a single mode but rather the sum of several phenomena (Liu 2012; Newman 2007)

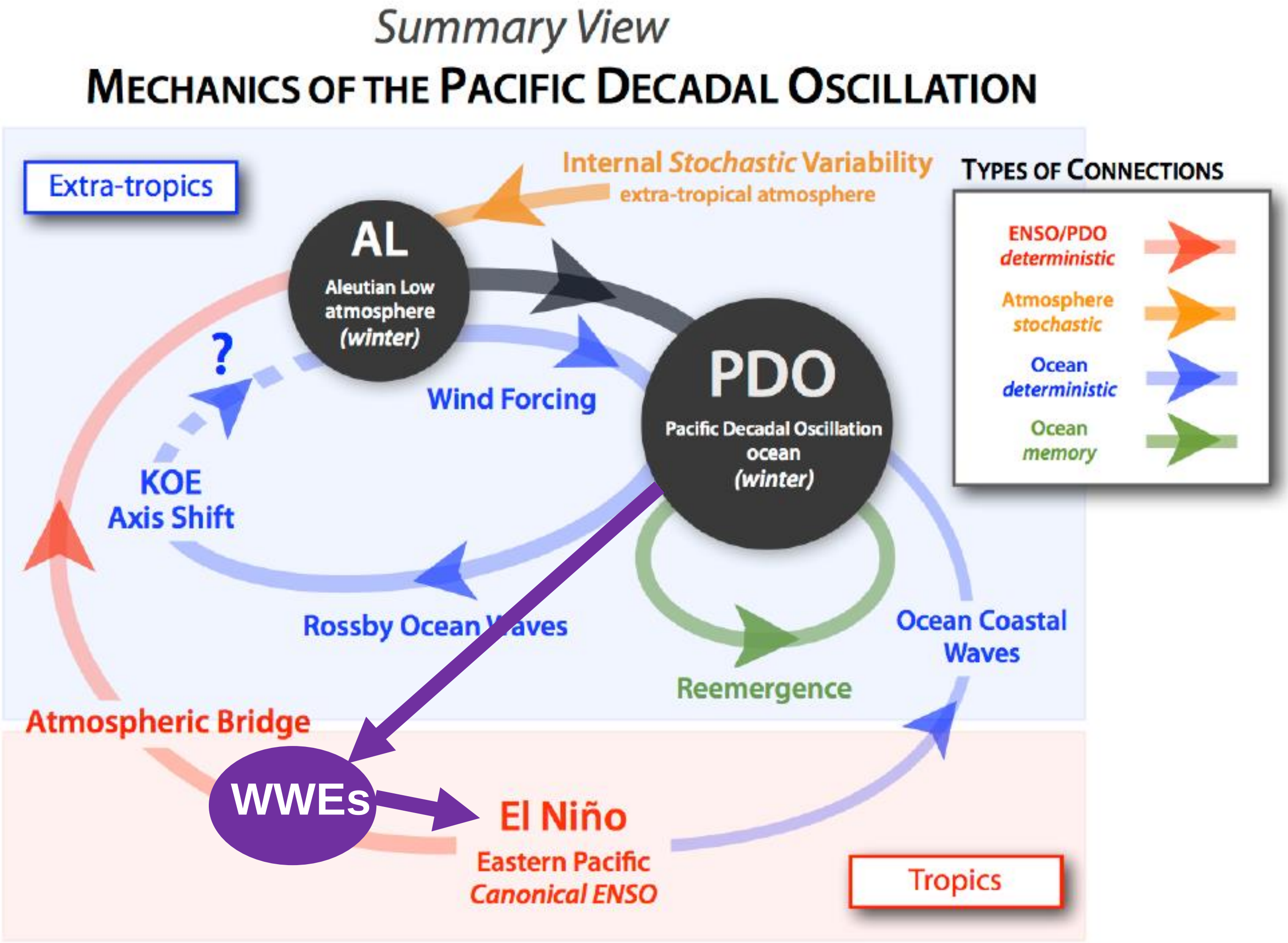

Figure 7. Summary figure of the basic processes involved in the PDO.

Newman et al. 2015

An inference …

- If what we think is somewhere nearly correct, then during +PDO we should have more extreme El Niño than during –PDO

- We looked at models in their multi-century runs.

Models	Length (years)	Length of +PDO/-PDO (years/years)	Frequency of strong El Niño (occurrences per 100 years)			
			+PDO Niño3 >1.5 s.d.	-PDO Niño3>1.5 s.d	+PDO Niño3 >2 s.d.	-PDO Niño3 >2 s.d.
bcc-csm1-1-m	390	199/191	8.54	4.19	3.52	1.05
bcc-csm1-1	490	252/238	5.16	7.15	2.38	1.26
CanESM2	490	256/234	8.59	2.56	2.73	0
CMCC-CESM	267	139/128	12.95	1.56	7.19	0.78
CMCC-CMS	490	238/252	13.45	1.59	5.88	0.40
CNRM-CM5	490	246/244	7.72	8.61	3.25	3.69
FGOALS-s2	490	250/240	10.40	4.58	5.20	2.08
GFDL-CM3	490	258/232	9.69	2.16	1.94	0.43
GFDL-ESM2G	490	258/232	9.69	3.45	5.04	0.43
GFDL-ESM2M	490	248/242	11.69	5.37	6.85	2.89
GISS-E2-H	490	248/242	4.84	8.68	1.21	2.89
GISS-E2-R	490	250/240	8.8	5.83	2.4	0.42
MIROC5	490	241/249	12.45	1.20	7.05	0
MPI-ESM-MR	490	244/246	7.79	4.88	2.46	1.63
MRI-CGCM3	490	246/244	8.54	4.92	2.03	2.87
NorESM1-M	490	251/239	10.76	2.93	3.98	1.26
NorESM1-ME	242	116/126	14.66	3.97	6.90	0.79
Average			9.75	4.33	4.12	1.35

Seasonal mean

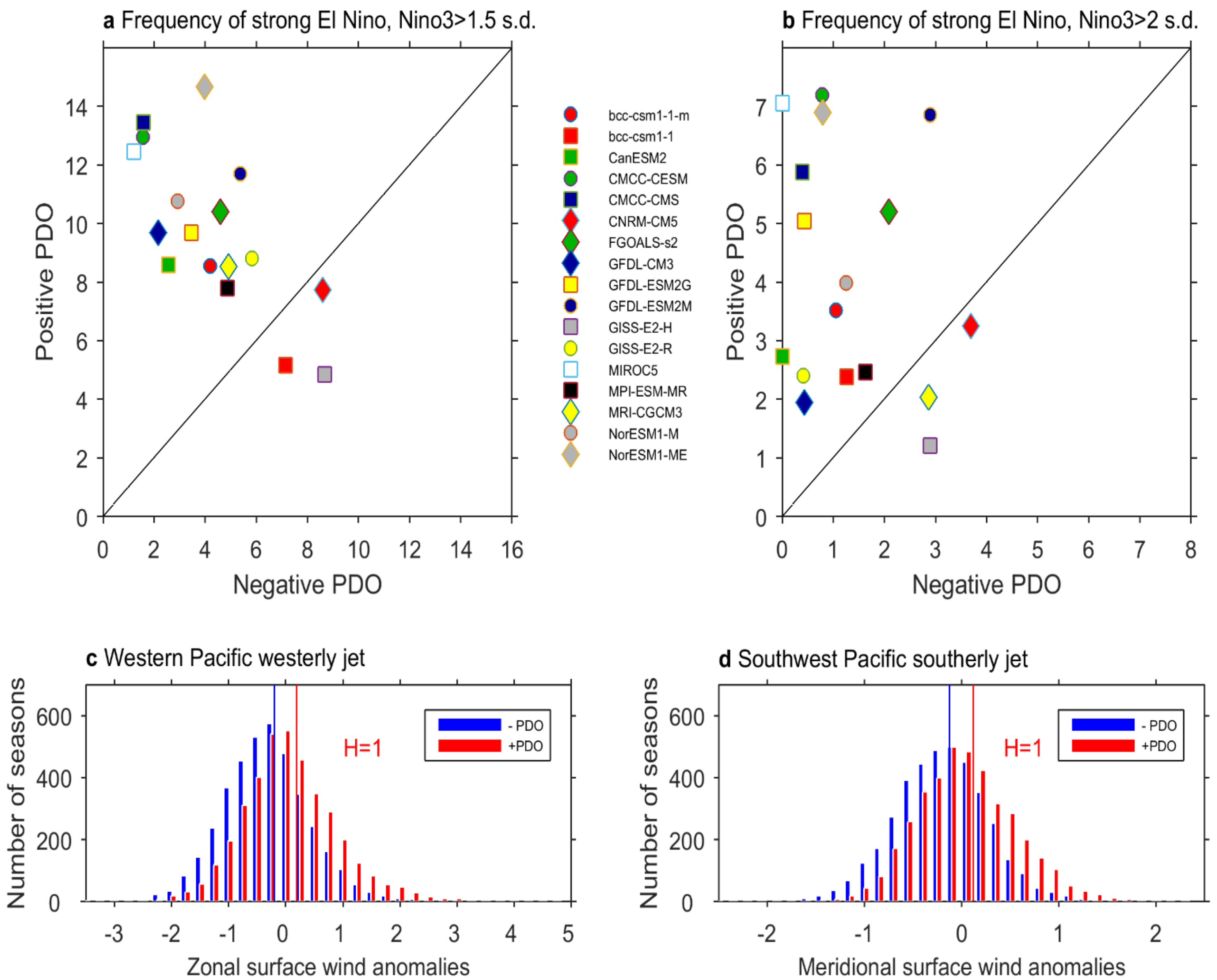

Supplementary Figure 2

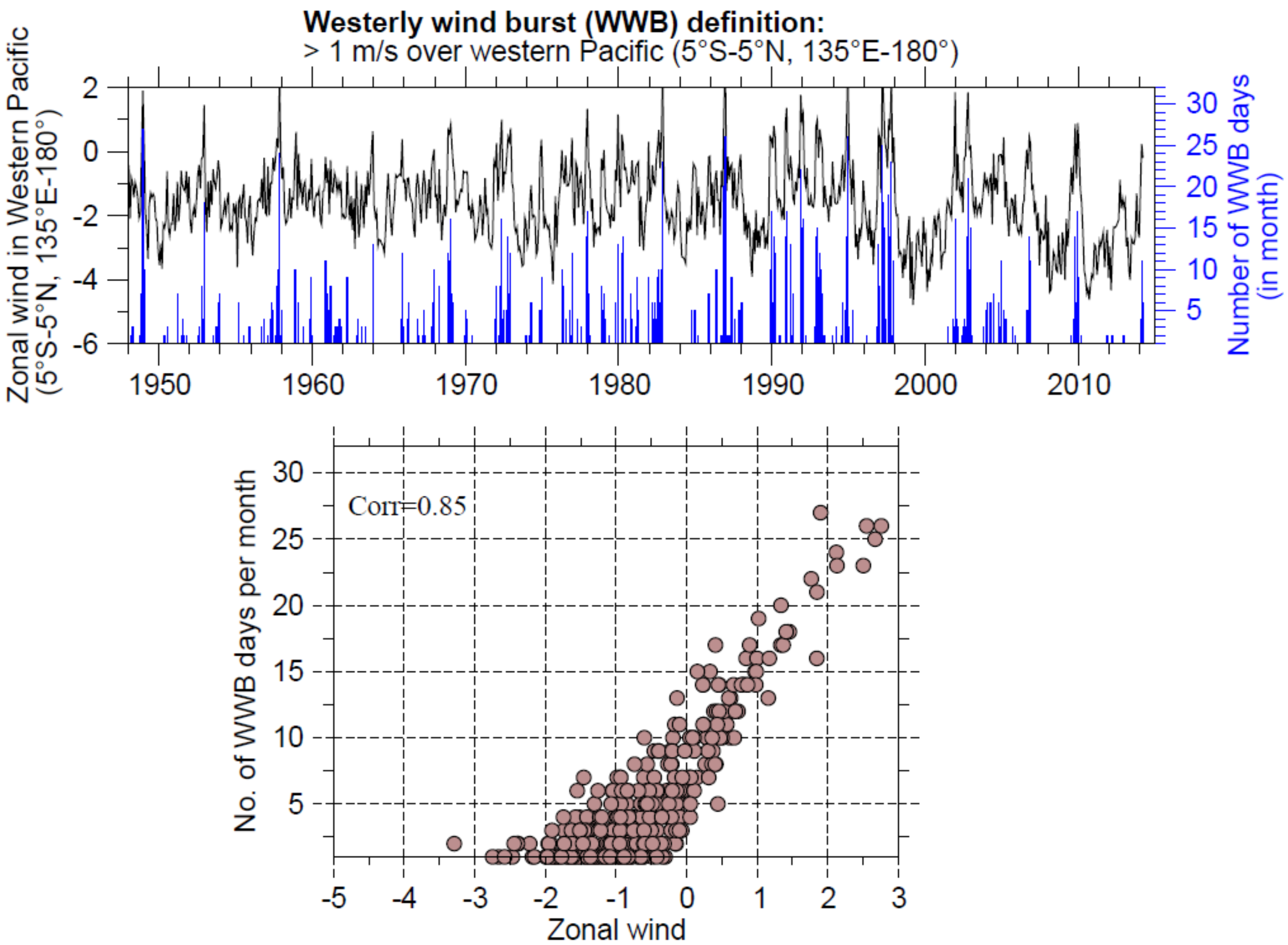

Summary + Implications

- +PDO is conducive to WWEs
- Because WWEs are coupled with El Niño anomalies
- and becauseEl Niño partially forces +PDO

a positive feedback operates between the PDO, WWEs, and El Niño

The current hiatus, in part driven by –PDO, is not conducive to extreme El Niño, which is a catalyst to end a hiatus, has the tendency to maintain itself.

Models that better simulate ENSO and WWEs will be more skilful for PDO prediction, and vice versa.

Thank you!

Contact: Wenju.cai@csiro.au

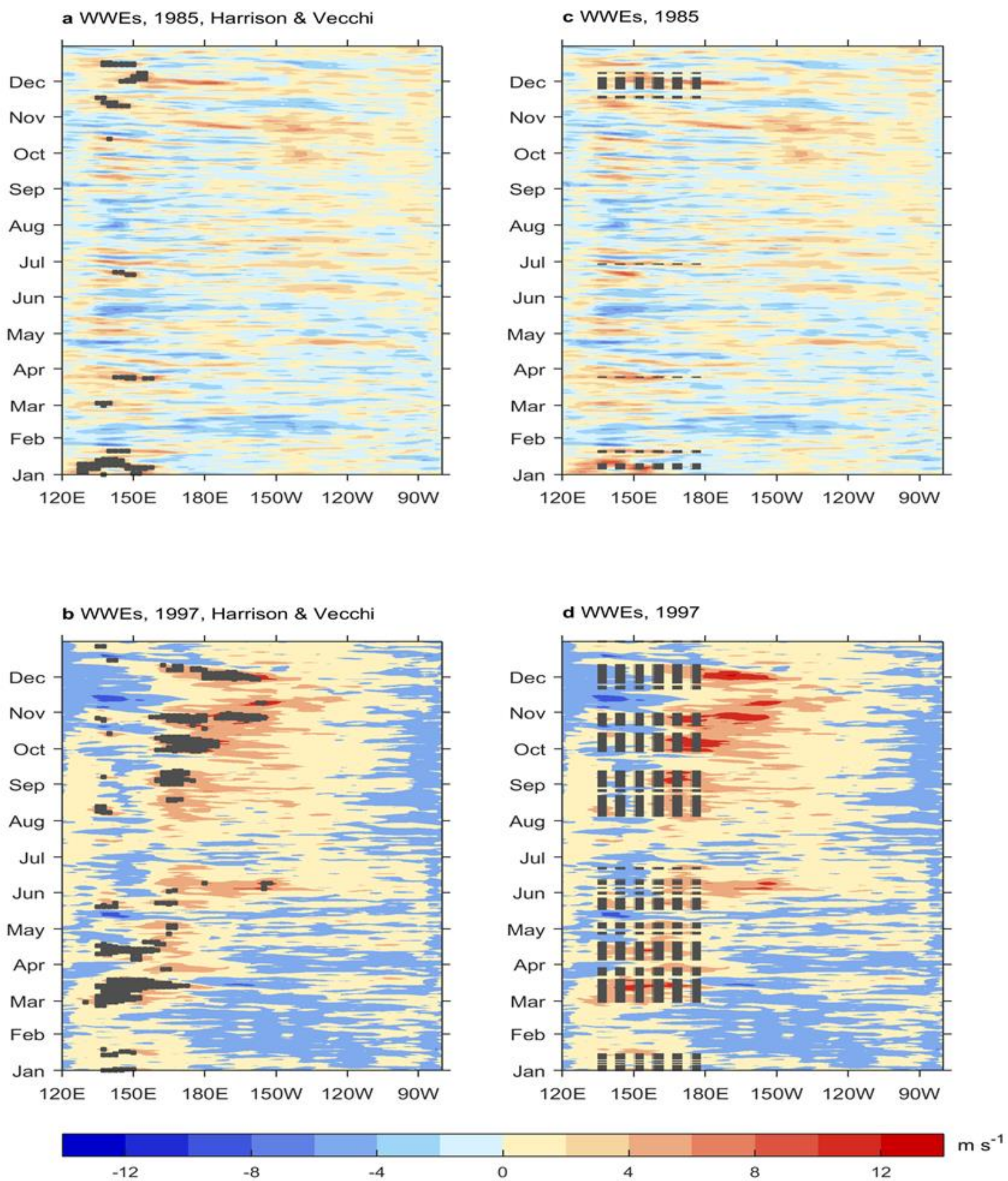

a WWEs, 1985, Harrison & Vecchi
c WWEs, 1985
b WWEs, 1997, Harrison & Vecchi
d WWEs, 1997
Dec
Nov
Oct
Sep
Aug
Jul
Jun
May
Apr
Mar
Feb
Jan
120E
150E
180E
150W
120W
90W
-12
-8
-4
0
4
8
12
m s-1

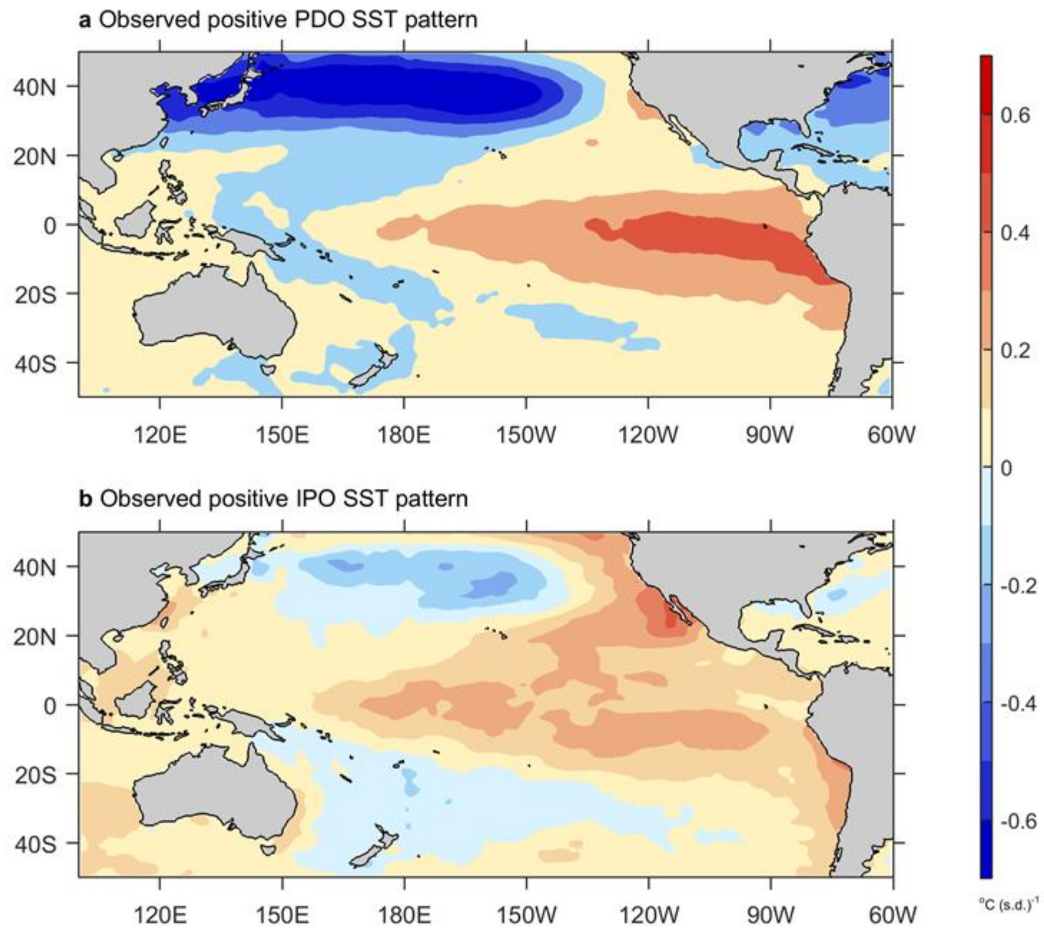
a Observed positive PDO SST pattern
40N
20N
0
20S
40S
120E
150E
180E
150W
120W
90W
60W
b Observed positive IPO SST pattern
0.6
0.4
0.2
0
-0.2
-0.4
-0.6
°C (s.d.)-1

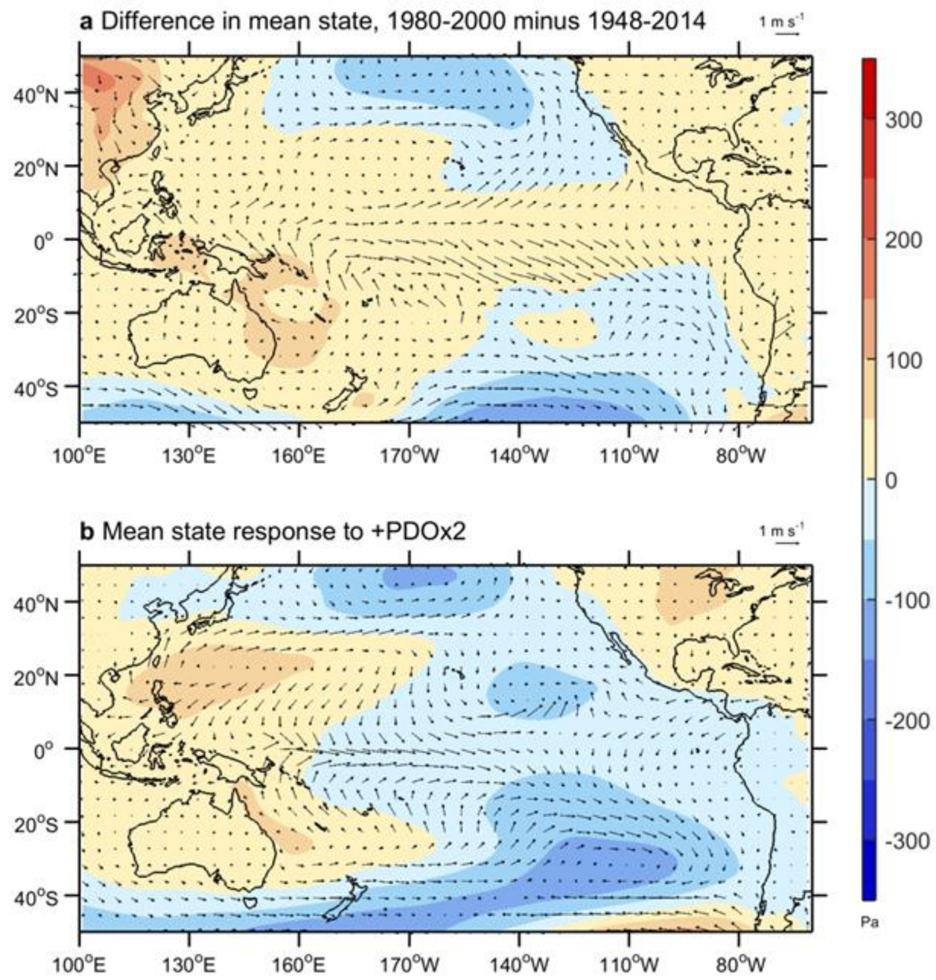
a Difference in mean state, 1980-2000 minus 1948-2014
1 m s-1
40°N
20°N
0°
20°S
40°S
100°E
130°E
160°E
170°W
140°W
110°W
80°W
b Mean state response to +PDOx2
1 m s-1
40°N
20°N
0°
20°S
40°S
100°E
130°E
160°E
170°W
140°W
110°W
80°W
300
200
100
0
-100
-200
-300
Pa

Supplementary Figure 2

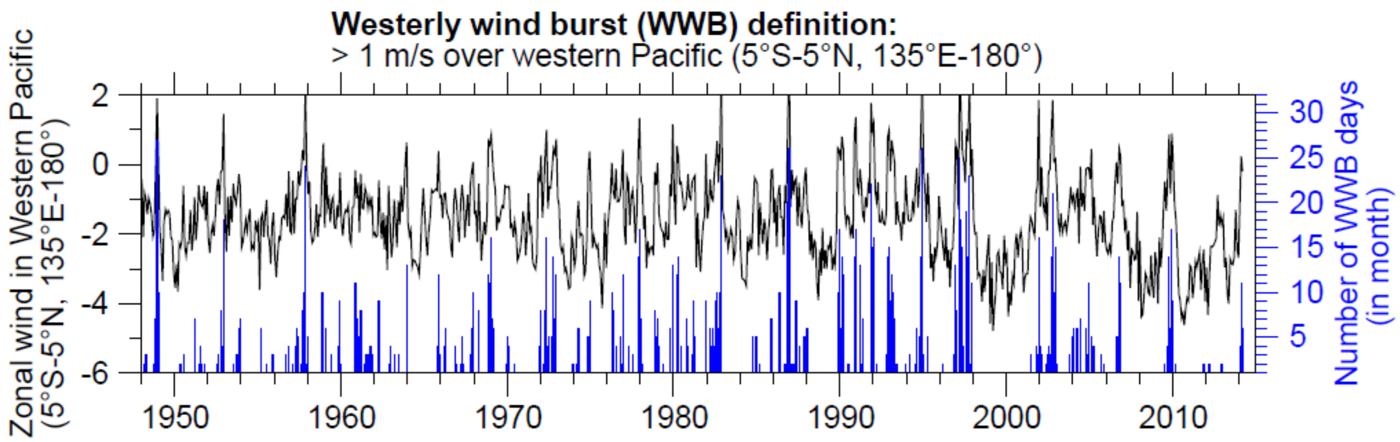

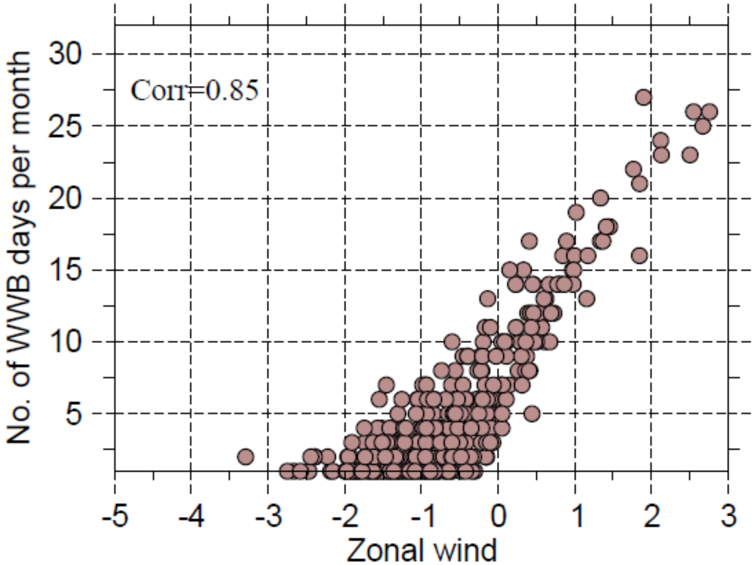

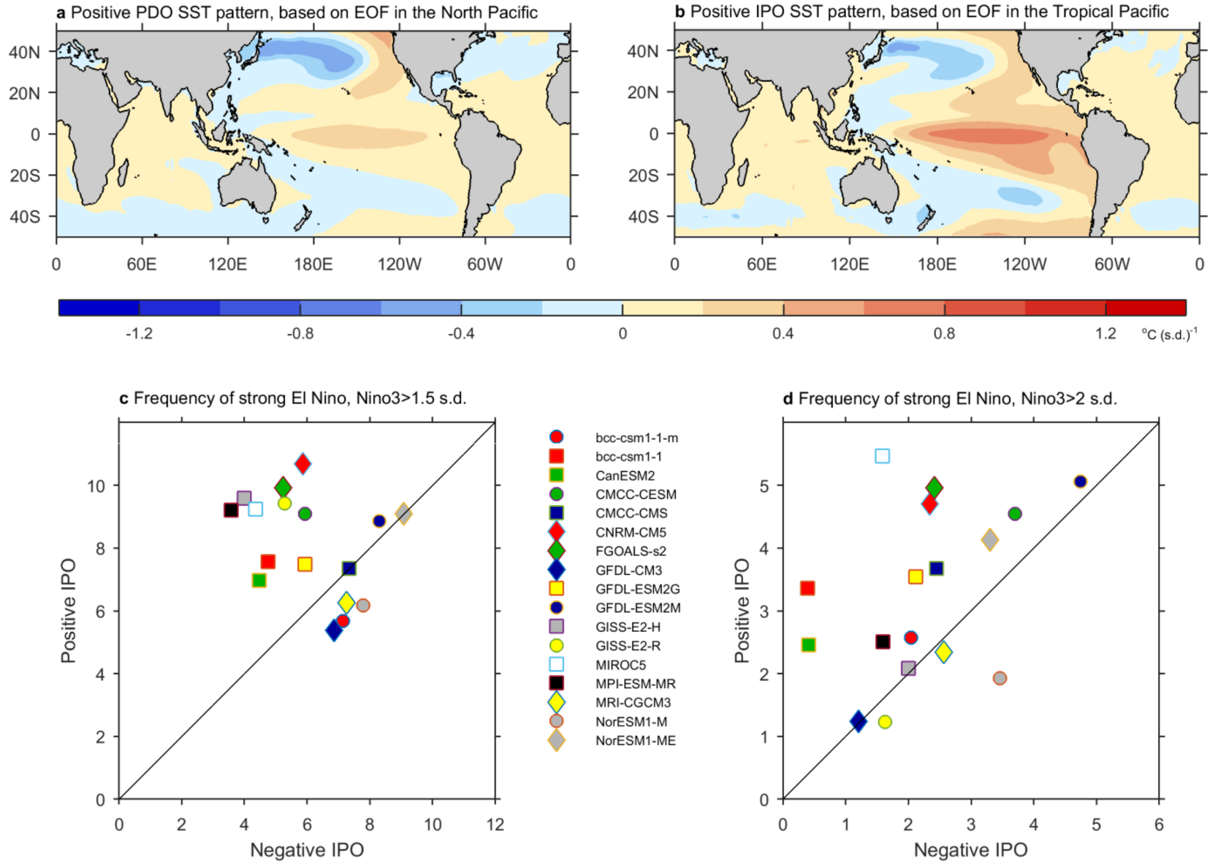
a Positive PDO SST pattern, based on EOF in the North Pacific
b Positive IPO SST pattern, based on EOF in the Tropical Pacific
40N
20N
0
20S
40S
0
60E
120E
180E
120W
60W
-1.2
-0.8
-0.4
0
0.4
0.8
1.2
°C (s.d.)-1
c Frequency of strong El Nino, Nino3>1.5 s.d.
d Frequency of strong El Nino, Nino3>2 s.d.
Positive IPO
Negative IPO
bcc-csm1-1-m
bcc-csm1-1
CanESM2
CMCC-CESM
CMCC-CMS
CNRM-CM5
FGOALS-s2
GFDL-CM3
GFDL-ESM2G
GFDL-ESM2M
GISS-E2-H
GISS-E2-R
MIROC5
MPI-ESM-MR
MRI-CGCM3
NorESM1-M
NorESM1-ME